Chapter 11.

Elastic and viscoplastic properties

R.A. Lebensohn
Los Alamos National Laboratory, US

Abstract

In this chapter, we review crystal elasticity and plasticity-based self-consistent theories and apply them to the determination of the effective response of polycrystalline aggregates. These mean-field formulations, which enable the prediction of the mechanical behaviour of polycrystalline aggregates based on the heterogeneous and/or directional properties of their constituent single crystal grains and phases, are ideal tools to establish relationships between microstructure and properties of these materials, ubiquitous among fuels and structural materials for nuclear systems.

Introduction

Mean-field theories linking microstructure and properties of heterogeneous materials can be used for the development of efficient algorithms for the prediction of the elastic and plastic response of polycrystals. In this chapter, we will review crystal elasticity and crystal plasticity-based self-consistent theories, and show applications of these formulations to the prediction of microstructure-property relations of polycrystalline aggregates.

The self-consistent (SC) approximation, one of the most commonly used homogenisation methods to estimate the mechanical response behaviour of polycrystals, was originally proposed by A.V. Hershey [3] for linear elastic materials. For nonlinear aggregates (as those formed by grains deforming in the viscoplastic regime), the several SC approximations that were subsequently proposed differ in the procedure used to linearise the local non-linear mechanical behaviour, but eventually all of them end up making use of the original linear SC theory. In general, SC estimates of the effective behaviour of heterogeneous materials are between the iso-strain upper-bound (i.e., Voigt and Taylor approximations in the elastic and viscoplastic regimes, respectively) and the iso-stress lower-bound (Reuss and Sachs approximations in the elastic and viscoplastic regimes, respectively).

This chapter is organised as follows: in Sections 2 and 3, we present the elastic self-consistent (ELSC) and viscoplastic self-consistent (VPSC) formulations, respectively. In Section 4, we show examples of the use of ELSC for the prediction of: (i) effective elastic behaviour of isotropic composites with increasing volume fractions of hard and soft phases, respectively and (ii) effective elastic anisotropy developing in an FCC polycrystal as crystallographic texture evolves. Finally, we show a classical benchmark for the different non-linear SC approaches in terms of the predicted effective behaviour of a random FCC polycrystal as a function of its rate-sensitivity.

Local constitutive behaviour and homogenisation

Let us consider a macroscopic strain $\mathbf{E}$ applied to an elastically heterogeneous material. The elastic behaviour at each material point $\mathbf{x}$ is given by:

$$\boldsymbol{\sigma}(\mathbf{x}) = \mathbf{C}^{(r)} : \boldsymbol{\varepsilon}(\mathbf{x}) \tag{1}$$

where $\mathbf{C}^{(r)}$ is the elastic stiffness of mechanical phase (r). Let us homogenise the behaviour of a linear heterogeneous medium whose local behaviour is described by Equation 1 by the following macroscopic linear relation:

$$\boldsymbol{\Sigma} = \overline{\mathbf{C}} : \mathbf{E} \tag{2}$$

where $\boldsymbol{\Sigma}$ and $\mathbf{E}$ are the effective stress and tensors, respectively, and $\overline{\mathbf{C}}$ is the stiffness of an a priori unknown Homogeneous Equivalent Medium (HEM). The problem underlying the SC method is that of an inhomogeneous domain (r) of modulus $\mathbf{C}^{(r)}$ embedded in an infinite medium of modulus $\overline{\mathbf{C}}$. Invoking the concept of the equivalent inclusion [13], the local constitutive behaviour in domain (r) can be rewritten as:

$$\boldsymbol{\sigma}(\mathbf{x}) = \overline{\mathbf{C}} : (\boldsymbol{\varepsilon}(\mathbf{x}) + \boldsymbol{\varepsilon}^*(\mathbf{x})) \tag{3}$$

where $\boldsymbol{\varepsilon}^*(\mathbf{x})$ is an eigenstrain field, which follows from replacing the inhomogeneity by an equivalent inclusion and the symbol "~" denotes local deviations from macroscopic values of the corresponding magnitudes. Using the equilibrium condition $\sigma_{ij,j}(\mathbf{x}) = 0$ and the relation $\tilde{\varepsilon}_{ij}(\mathbf{x}) = \frac{1}{2}\left(\tilde{u}_{i,j}(\mathbf{x}) + \tilde{u}_{j,i}(\mathbf{x})\right)$ between the strain and displacement gradient fields we obtain:

$$\overline{C}_{ijkl}\, \tilde{u}_{k,lj}(\mathbf{x}) + \varphi_{ij,j}(\mathbf{x}) = 0 \tag{4}$$

where:

$$\varphi(\mathbf{x}) = -\overline{\mathbf{C}} : \boldsymbol{\varepsilon}^*(\mathbf{x}) \tag{5}$$

is a polarisation field. Differential Equation 5 can be solved using the Green function method. If $G_{km}(\mathbf{x})$ is the Green function associated with $\tilde{u}_k(\mathbf{x})$, which solves the auxiliary problem of a unitary volumetric force, with a single non-vanishing m-component:

$$\overline{C}_{ijkl}\, G_{km,lj}(\mathbf{x} - \mathbf{x}') + \delta_{im}\, \delta(\mathbf{x} - \mathbf{x}') = 0 \tag{6}$$

Once the solution of Equation 7 is obtained, the displacement:

$$\tilde{u}_k(\mathbf{x}) = \int_{R^3} G_{ki}(\mathbf{x}-\mathbf{x}')\, f_i(\mathbf{x}')\, d\mathbf{x}'$$

$$\tilde{u}_{k,l}(\mathbf{x}) = \int_{R^3} G_{ki,jl}(\mathbf{x}-\mathbf{x}')\, \varphi_{ij}(\mathbf{x}')\, d\mathbf{x}'$$

An inclusion of volume Ω in an infinite medium takes the form:

$$\tilde{u}^{(r)}_{k,l} = \left(-\frac{1}{\Omega} \int_{\Omega\Omega} G_{ki,jl}(\mathbf{x}-\mathbf{x}')\, d\mathbf{x}\, d\mathbf{x}' \right) \overline{C}_{ijmn} \varepsilon^{*(r)}_{mn} \tag{7}$$

where $\tilde{u}^{(r)}_{k,l}$ and $\varepsilon^{*(r)}_{mn}$ are averages inside the inclusion and the expression of tensor T_{klij} solution of the above integral expression, can be found in [1].

The Eshelby tensor, a function of $\overline{\mathbf{C}}$ and the shape of the ellipsoidal inclusion, is given by:

$$S_{ijkl} = \frac{1}{4}\left(T_{ijmn} + T_{jimn} + T_{ijnm} + T_{jinm}\right)\overline{C}_{mnkl} \tag{8}$$

Thus, taking symmetric part in Equation 9 gives:

$$\tilde{\boldsymbol{\varepsilon}}^{(r)} = \mathbf{S} : \boldsymbol{\varepsilon}^{*(r)} \tag{9}$$

Interaction, localisation and self-consistent equations

Taking volume averages over the domain of the inclusion on both sides of Equation 4 and replacing the eigenstrain given by Equation 10, we obtain the interaction equation:

$$\tilde{\boldsymbol{\sigma}}^{(r)} = -\overline{\mathbf{C}} : \mathbf{S}^{-1} : (\mathbf{I}-\mathbf{S})\tilde{\boldsymbol{\varepsilon}}^{(r)} = -\tilde{\mathbf{C}} : \tilde{\boldsymbol{\varepsilon}}^{(r)} \tag{10}$$

Replacing the constitutive relations of the inclusion and the effective medium in the latter and after some manipulation, one can write the following localisation equation:

$$\boldsymbol{\varepsilon}^{(r)} = \left(\mathbf{C}^{(r)} + \tilde{\mathbf{C}}\right)^{-1} : \left(\overline{\mathbf{C}} + \tilde{\mathbf{C}}\right) : \mathbf{E} = \mathbf{A}^{(r)} : \mathbf{E} \tag{11}$$

The previous solution for an equivalent inclusion embedded in an effective medium can be used to construct a homogenisation model, consisting in regarding each mechanical phase (r) as heterogeneity embedded in an effective medium that represents the polycrystal. The properties of such medium are not known *a priori* but have to be found through an iterative procedure. Replacing the stress localisation equation (Equation 11) in the averaged local constitutive equation (Equation 1) we obtain:

$$\boldsymbol{\sigma}^{(r)} = \mathbf{C}^{(r)} : \mathbf{A}^{(r)} : \boldsymbol{\Sigma} \tag{12}$$

Taking volumetric average (denoted <.>), enforcing the condition that the average stress over the aggregate has to coincide with the corresponding macroscopic magnitude and using the macroscopic constitutive relation (Equation 2), we obtain the following self-consistent equation for the HEM's stiffness:

$$\overline{\mathbf{C}} = \left\langle \mathbf{C}^{(r)} : \mathbf{A}^{(r)} \right\rangle \tag{13}$$

To illustrate the use of this ELSC formulation, we describe here the steps required to predict the local and overall elastic response of an elastically heterogeneous materials. We start, for convenience, from an initial Voigt guess, i.e.: $\boldsymbol{\varepsilon}^{(r)} = \mathbf{E}$ for all phases, and:

$\overline{\mathbf{C}} = \langle \mathbf{C}^{(r)} \rangle$. Next, the Eshelby tensor **S** can be calculated for the ellipsoidal shape of the mechanical phases. Subsequently, the interaction tensor $\widetilde{\mathbf{C}}$ (Equation 10), and the localisation tensors $\mathbf{A}^{(r)}$ for each phase (Equation 11), are obtained. With these, an improved estimate of $\overline{\mathbf{C}}$ can be calculated, using the self-consistent fix-point equation (Equation 13). After achieving convergence on the macroscopic stiffness (and, consequently, also on the interaction and localisation tensors), a new estimation of average grain strain and stresses can be obtained, e.g., using the localisation relation and the averaged local constitutive equation (Equation 1).

Viscoplastic self-consistent method

In what follows, the SC formalism described in the previous section will be extended to the case of viscoplastic polycrystals. Each SR grain will be treated as an ellipsoidal viscoplastic inclusion embedded in an effective viscoplastic medium. Deformation in the grains is accommodated by dislocation glide activated by a resolved shear stress.

Local constitutive behaviour, linearisation and homogenisation

Let us consider that a macroscopic strain-rate $\dot{\mathbf{E}}$ is applied to the polycrystal. Let us assume that the plastic component of the deformation is much larger than the elastic part and therefore the flow is incompressible. The viscoplastic constitutive behaviour at each material point is described by means of the following non-linear, rate-sensitive equation:

$$\dot{\boldsymbol{\varepsilon}}(\mathbf{x}) = \sum_{k=1}^{N_k} \mathbf{m}^k(\mathbf{x})\dot{\gamma}^k(\mathbf{x}) = \dot{\gamma}_o \sum_{k=1}^{N_k} \mathbf{m}^k(\mathbf{x}) \left(\frac{\left|\mathbf{m}^k(\mathbf{x}):\boldsymbol{\sigma}'(\mathbf{x})\right|}{\tau_o^k(\mathbf{x})} \right)^n \times \mathrm{sgn}\left(\mathbf{m}^k(\mathbf{x}):\boldsymbol{\sigma}'(\mathbf{x})\right) \tag{14}$$

where the sum runs over all N_k slip and twinning systems. τ_0^k and $\mathbf{m}^k(\mathbf{x}) = \frac{1}{2}\left(\mathbf{n}^k(\mathbf{x}) \otimes \mathbf{b}^k(\mathbf{x}) - \mathbf{b}^k(\mathbf{x}) \otimes \mathbf{n}^k(\mathbf{x})\right)$ are the threshold resolved shear stress and the symmetric Schmid tensor associated with slip or twinning system (k) (with $\mathbf{n}^k$ and $\mathbf{b}^k$ being the normal and Burgers vector direction of such slip or twinning system), $\dot{\boldsymbol{\varepsilon}}$ and $\boldsymbol{\sigma}'$ are the deviatoric strain-rate and stress tensors, $\dot{\gamma}^k$ is the local shear-rate on slip or twinning system (k), $\dot{\gamma}_0$ is a normalisation factor and *n* is the rate-sensitivity exponent.

Let us assume that the following linear relation (i.e., an approximation of the actual non-linear relation, Equation 26) holds between the strain-rate and stress in the SR grain (r):

$$\dot{\boldsymbol{\varepsilon}}(\mathbf{x}) = \mathbf{M}^{(r)} : \boldsymbol{\sigma}'(\mathbf{x}) + \dot{\boldsymbol{\varepsilon}}^{o(r)} \tag{15}$$

where $\mathbf{M}^{(r)}$ and $\dot{\boldsymbol{\varepsilon}}^{o(r)}$ are respectively a viscoplastic compliance and a back-extrapolated term (stress-free strain-rate) of SR grain (r). Different choices are possible for the linearised behaviour at grain level, and the results of the homogenisation scheme depend on this choice. The *secant approximation* [4,5]consists in assuming $\dot{\boldsymbol{\varepsilon}}_{sec}^{o(r)} = 0$, and the following linearised modulus:

$$\mathbf{M}_{sec}^{(r)} = \dot{\gamma}_o \sum_k \frac{\mathbf{m}^{k(r)} \otimes \mathbf{m}^{k(r)}}{\tau_o^{k(r)}} \left(\frac{\mathbf{m}^{k(r)} : \boldsymbol{\sigma}'^{(r)}}{\tau_o^{k(r)}} \right)^{n-1} \tag{16}$$

where the index (r) in $\mathbf{m}^{k(r)}$ and $\tau_o^{k(r)}$ indicates uniform (average) values of these magnitudes, corresponding to a given orientation and hardening state associated with SR grain (r). Under the *affine approximation* [10], the moduli are given by:

$$\mathbf{M}_{aff}^{(r)} = n\dot{\gamma}_o \sum_k \frac{\mathbf{m}^{k(r)} \otimes \mathbf{m}^{k(r)}}{\tau_o^{k(r)}} \left(\frac{\mathbf{m}^{k(r)} : \boldsymbol{\sigma}'^{(r)}}{\tau_o^{k(r)}} \right)^{n-1} \tag{17}$$

$$\dot{\boldsymbol{\varepsilon}}_{aff}^{o(r)} = (1-n)\dot{\gamma}_o \sum_k \left(\frac{\mathbf{m}^{k(r)} : \boldsymbol{\sigma}'^{(r)}}{\tau_o^{k(r)}} \right)^{n} \times \mathrm{sgn}\left(\mathbf{m}^{k(r)} : \boldsymbol{\sigma}'^{(r)} \right) \tag{18}$$

The secant and affine models, together the *tangent approximation* of A. Molinari et al. [11] and R.A. Lebensohn et al. [6] (which combines aspects of the former two), [8] are first-order approximations, since they are based on linearisation schemes that at grain level make use of information on field averages only, disregarding higher-order statistical information inside the SR grains. However, the above assumption may be not sufficient, especially when strong directionality and/or large variations in local properties are to be expected. To overcome the above limitations, P. Ponte Castañeda et al. have developed more accurate nonlinear homogenisation methods, using linearisation schemes at grain level that also incorporate information on the second moments of the field fluctuations in the mechanical phases. These more elaborate SC formulations are based on the use of so-called linear comparison methods, which express the effective potential of the nonlinear VP polycrystal in terms of that of a linearly viscous aggregate with properties that are determined from suitably-designed variational principles [2,9,14,15]. Once a specific type of linearisation is chosen, the viscoplastic self-consistent method can be constructed following similar procedure as in the elastic case. The homogenised behaviour is given by Equation 2:

$$\dot{\mathbf{E}} = \overline{\mathbf{M}} : \boldsymbol{\Sigma}' + \dot{\mathbf{E}}^{o} \tag{19}$$

where $\dot{\mathbf{E}}$ and $\boldsymbol{\Sigma}'$ are the macroscopic deviatoric strain-rate and stress tensors and $\overline{\mathbf{M}}$ and $\dot{\mathbf{E}}^{0}$ are respectively the compliance and back-extrapolated term of the *a priori*

unknown viscoplastic HEM. The average strain-rate deviation in the ellipsoidal domain $\tilde{\dot{\boldsymbol{\varepsilon}}}^{(r)} = \dot{\mathbf{E}} - \dot{\boldsymbol{\varepsilon}}^{(r)}$ is given by Equation 9:

$$\tilde{\dot{\boldsymbol{\varepsilon}}}^{(r)} = \mathbf{S} : \dot{\boldsymbol{\varepsilon}}^{*(r)} \tag{20}$$

The interaction equation is given by Equation 10:

$$\tilde{\dot{\boldsymbol{\varepsilon}}}^{(r)} = -(\mathbf{I} - \mathbf{S})^{-1} : \mathbf{S} : \overline{\mathbf{M}} : \tilde{\boldsymbol{\sigma}}'^{(r)} = -\tilde{\mathbf{M}} : \tilde{\boldsymbol{\sigma}}'^{(r)} \tag{21}$$

The localisation equation is then written as Equation 11:

$$\boldsymbol{\sigma}'^{(r)} = \left(\mathbf{M}^{(r)} + \tilde{\mathbf{M}}\right)^{-1} \left(\left(\overline{\mathbf{M}} + \tilde{\mathbf{M}}\right) : \boldsymbol{\Sigma}' + \left(\dot{\mathbf{E}}^{o} - \dot{\boldsymbol{\varepsilon}}^{o(r)}\right)\right) = \mathbf{B}^{(r)} : \boldsymbol{\Sigma}' + \mathbf{b}^{(r)} \tag{22}$$

The self-consistent equations are then given by Equation 13:

$$\overline{\mathbf{M}} = \left\langle \mathbf{M}^{(r)} : \mathbf{B}^{(r)} \right\rangle \text{ and } \dot{\mathbf{E}}^{o} = \left\langle \mathbf{M}^{(r)} : \mathbf{b}^{(r)} + \dot{\boldsymbol{\varepsilon}}^{o(r)} \right\rangle \tag{23}$$

Numerical implementation

Starting, e.g., from an initial Taylor guess: $\dot{\boldsymbol{\varepsilon}}^{(r)} = \dot{\mathbf{E}}$ for all grains, a non-linear equation can be solved to get $\boldsymbol{\sigma}'^{(r)}$ and, using an appropriate linearisation scheme, the initial values of $\mathbf{M}^{(r)}$ and $\dot{\boldsymbol{\varepsilon}}^{o(r)}$ can be obtained, for each SR grain (r). Next, initial guesses for the macroscopic moduli $\overline{\mathbf{M}}$ and $\dot{\mathbf{E}}^{O}$ can be obtained as simple averages of the local moduli. With them and the applied strain-rate, the initial guess for the macroscopic stress $\boldsymbol{\Sigma}'$ can be obtained. The Eshelby tensors can be calculated using the macroscopic moduli and the ellipsoidal shape of the SR grains. Subsequently, the interaction tensor (Equation 21), and the localisation tensors (Equation 22), can be calculated as well, and new estimates of the macroscopic moduli can be obtained, by solving iteratively the self-consistent equation (Equation 23). After achieving convergence on the macroscopic moduli (and, consequently, also on the macroscopic stress and the interaction and localisation tensors), a new estimation of the average grain stresses is obtained, using the localisation relation. If the recalculated average grain stresses are different (within certain tolerance) from the input values, a new iteration should be started, until convergence is reached.

Applications

We show an application of the ELSC model to the prediction of the effective elastic shear modulus of isotropic two-phase composites made of: phase #1 with shear modulus and Poisson ratio $\mu_1 = 1$ and $\nu_1 = 1/3$, and phase #2 being either a hard phase with $\mu_2 = 100$ and $\nu_2 = 1/3$, or a void phase, i.e. $\mu_2 = 0$. Figure 1, corresponding to the case of equiaxed phase morphologies, shows the shear modulus of the composite as a function of phase #2 content. Together with the ELSC estimate, we show the Voigt, Reuss and Hill (defined as the arithmetic average between the Reuss and Voigt values) predictions. From Figure 1a (phase #2 100 times harder than phase #1) shows the huge spread existing between the bounds, and also the large difference between the SC estimate and the Hill average. Figure 1b (phase #2 void) shows similar results, as well as the "percolation limit"

of the SC theory at 50% volume fraction, at which the presence of a void phase determines a vanishing load-bearing capacity of the aggregate.

Figure 1. Voigt, Reuss, Hill and ELSC predictions of the effective shear modulus as a function of phase #2 content (x_2), for isotropic two-phase composites made of phase #1 with shear modulus and Poisson ratio $\mu_1 = 1$ and $\nu_1 = 1/3$, and phase #2 being either: a) a hard phase with $\mu_2 = 100$ and $\nu_2 = 1/3$, and b) a void phase, i.e., $\mu_2 = 0$

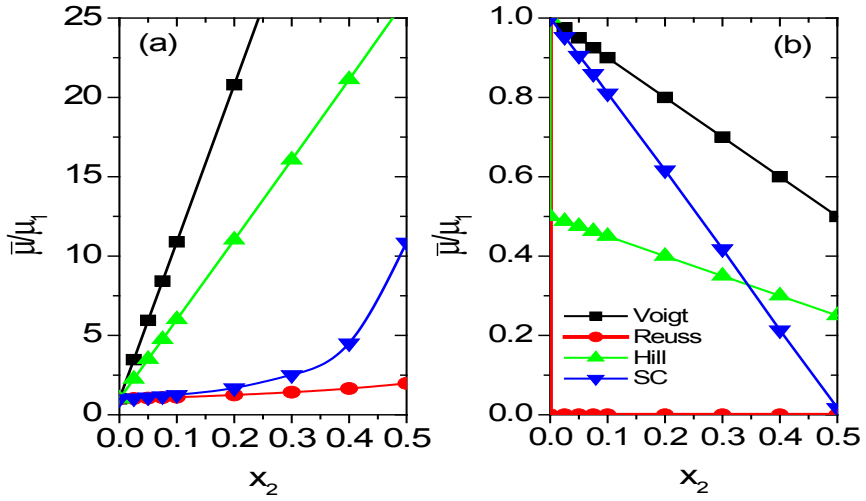

All cases correspond to equi-axed phase morphologies.

Figure 2 exemplifies how the ELSC formulation naturally captures the effect of morphologic anisotropy. The cases shown correspond to the same materials as before, except that the morphology of the phases is represented by oblate spheroids with their short axis 10 times shorter that the long ones aligned with direction x_3. It can be seen that: (i) the (isotropic) elastic constants for the homogeneous phase #1 material are $C_{11} = C_{22} = C_{33} = 4$, $C_{12} = C_{13} = C_{23} = 2$ and $C_{44} = C_{55} = C_{66} = 1$, and (ii) the effective response predicted by ELSC (unlike the Voigt, Reuss and Hill predictions) are anisotropic (axisymmetric), e.g., in Figures 2a and 2d (hard and soft phase #2, respectively), note the very different evolution of the directional moduli $C_{11} (= C_{22})$ along the long morphologic directions, with respect to C_{33}, giving the response along the short direction.

Texture-induced anisotropy is also captured by the ELSC approach. Figure 3 shows the evolution of the nine independent orthotropic elastic constants for the case plane strain deformation (extension along x_1 and shortening along x_3) of an initially random austenitic steel polycrystal (single crystal elastic constants: $C_{11} = 204.6\ \text{GPa}$, $C_{12} = 137.7\ \text{GPa}$ and $C_{44} = 126.2\ \text{GPa}$) as a function of the true strain along x_1 (texture evolution calculated with the affine VPSC approach). It should be noted that the orthotropic symmetry and relative values of the polycrystal elastic constants follow naturally from the texture evolution, e.g., the prediction of $C_{22} > C_{11} > C_{33}$ reflects the strong alignment of the hard <111> crystallographic directions with x_2 as texture evolves.

Figure 2. Same as Figure 1, except that the morphology of the phases is represented by oblate spheroids with their short axis ten times shorter that the long ones aligned with direction x_3

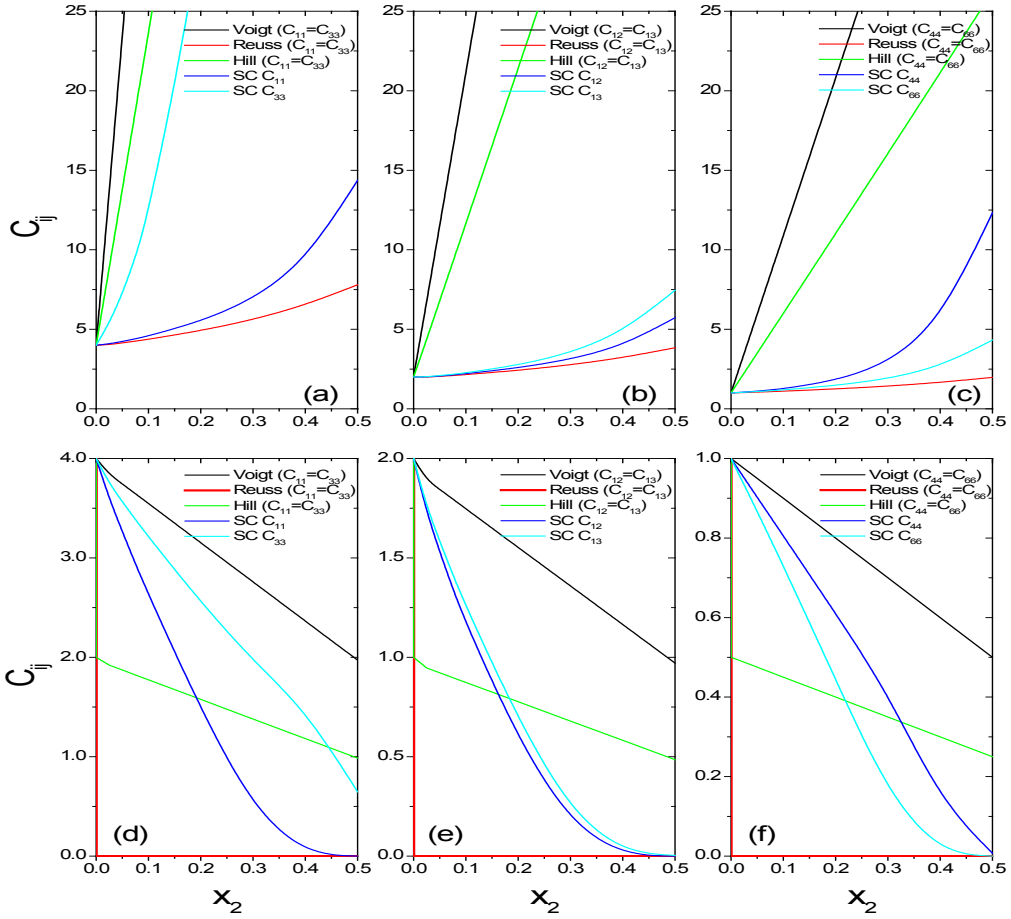

Upper row: case of hard phase #2, lower row: case of voided phase #2. a,d) C_{11}, C_{22}, C_{33}, b,e), C_{12}, C_{13}, C_{23} and c,f) C_{44}, C_{55}, C_{66}.

The advantage of SC schemes to get improved predictions of the mechanical behaviour of viscoplastic polycrystals, becomes evident as the contrast in local properties increases. The prediction of the effective properties of a random FCC polycrystal as the rate-sensitivity of the material changes is a classical benchmark for the different non-linear SC approaches. Figure 4 shows a comparison between average Taylor factor vs. rate-sensitivity ($1/n$) curves, for a random FCC polycrystal under uniaxial tension [8]. The Taylor factor is calculated as Σ_{eq}^{ref}/τ_o, where τ_0 is the threshold stress of the (111)<110> slip systems, and Σ_{eq}^{ref} is the macroscopic equivalent stress corresponding to an applied uniaxial strain-rate with a Von Mises equivalent value $E_{eq}^{ref}=1$.

Figure 3. Evolution of the nine independent orthotropic elastic constants for the case of plane strain deformation of an initially random austenitic steel polycrystal, as a function of the true strain along the extension direction x_1

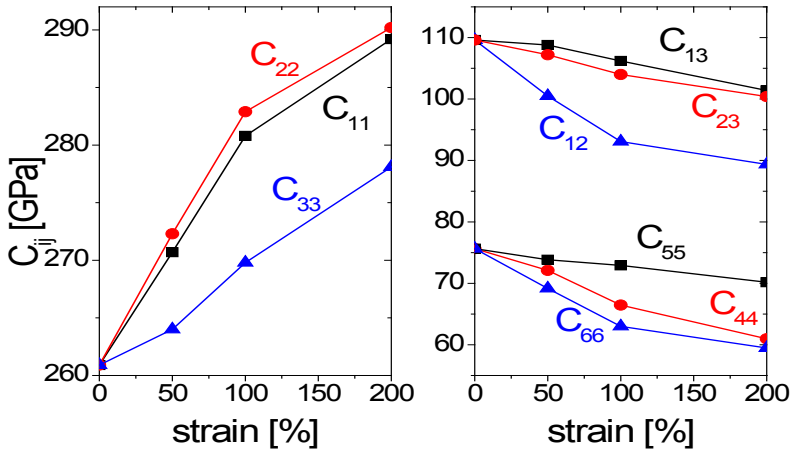

The curves in Figure 4 correspond to the Taylor model, the different first-order SC approximations, and the second-order procedure [9]. The solid star indicates the rate-insensitive Sachs lower-bound. The open stars correspond to reference solutions, obtained from ensemble averages of full-field solutions performed on random polycrystals using a Fast Fourier Transform-based method [12,7]. These ensemble averages were calculated over the outcome of "numerical experiments" performed on 100 unit cells generated alike, i.e., by random assignation of orientations to a given array of grains, but which differ at micro level due to the inherent stochastic character of such generation procedure. The averages over a sufficiently large number of configurations should give the effective properties of a polycrystal with random microstructure. From the comparison between the different mean-field and the full-field estimates, it can be observed that: (i) the Taylor approach gives the stiffest response, consistent with the upper-bound character of this model; (ii) all the SC estimates coincide for n=1, i.e., the linear SC case; (iii) in the rate-insensitive limit, the secant and tangent models tend to the upper- and lower-bounds, respectively, while the affine and second-order approximations remain intermediate with respect to the bounds; (iv) the best match with the exact solutions corresponds to the second-order approach.

Figure 4. Average Taylor factor for a random FCC polycrystal under uniaxial tension, calculated with the different SC approaches (lines+symbols) and reference values (stars) obtained by means of ensemble averages of full-field solutions [8]

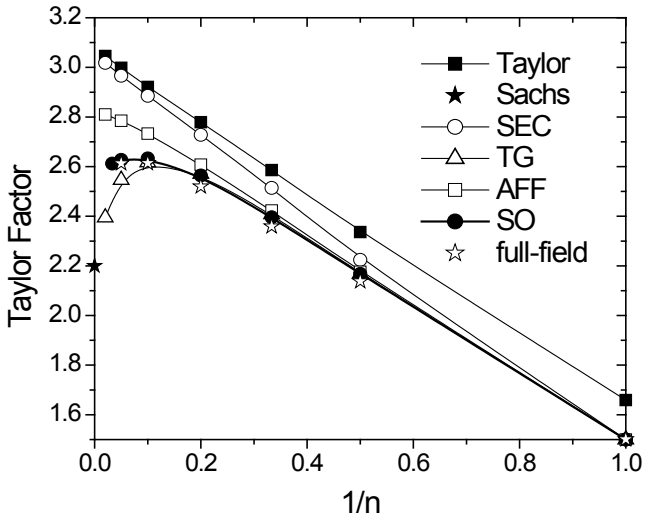

Conclusion and future challenges

We have presented the ELSC and VPSC formulations, and exemplified their use to establish relationships between microstructure and properties of composites and polycrystalline materials. The elastic model is a mature formulation that can be readily applied to fuels and structural materials for nuclear systems to predict effective elastic properties if the single crystal elastic constants, morphology, texture and phase distribution are known. The viscoplastic model can be applied to predict the effective anisotropic plastic response as a function of single crystal plastic properties and morphologic and crystallographic texture. For other inelastic deformation regimes of relevance, like thermal and irradiation creep, the formulation should be modified with pertinent constitutive relations at grain level (Equation 14) that reflect the single crystal response in such regimes. The presented methodology can be applied to predict the effective behaviour of polycrystalline aggregates deformation in such regimes.

References

[1] Berveiller, M., O. Fassi-Fehri, A. Hihi (1987), "The problem of 2 plastic and heterogeneous inclusions in an anisotropic medium", *International Journal of Engineering Science*, 25, 691-709.

[2] de Botton, G., P. Ponte Castañeda (1995), "Variational estimates for the creep-behavior of polycrystals", *Proceedings of the Royal Society of London A*, 448, 121-142.

[3] Hershey, A.V. (1954), "The elasticity of an isotropic aggregate of anisotropic cubic crystals", *Journal of Applied Mechanics*, 21, 236-240.

[4] Hill, R. (1965), "Continuum micro-mechanics of elastoplastic polycrystals", *Journal of the Mechanics and Physics of Solids,* 13, 89.

[5] Hutchinson, J.W. (1976), "Bounds and self-consistent estimates for creep of polycrystalline materials", *Proceedings of the Royal Society of London A*, 348, 101-127.

[6] Lebensohn, R.A. et al. (1993), "A self-consistent approach for the simulation of plastic deformation and texture development of polycrystals: Application to zirconium alloys", *Acta Metallurgica et Materialia*, 41, 2611-2624.

[7] Lebensohn, R.A. (2001), "N-site modelling of a 3D viscoplastic polycrystal using Fast Fourier Transform", *Acta Materialia*, 49, 2723-2737.

[8] Lebensohn, R.A. et al. (2007), "Self-consistent modeling of the mechanical behavior of viscoplastic polycrystals incorporating intragranular field fluctuations", *Philosophical Magazine*, 87, 4287-4322.

[9] Liu, Y., P. Ponte Castañeda (2004), "Second-order theory for the effective behavior and field fluctuations in viscoplastic polycrystals", *Journal of the Mechanics and Physics of Solids*, 52, 467-495.

[10] Masson, R. et al. (2000), "Affine formulation for the prediction of the effective properties of nonlinear composites and polycrystals", *Journal of the Mechanics and Physics of Solids,* 48, 1203-1227.

[11] Molinari, A. et al. (1987), "Self consistent approach of the large deformation polycrystal viscoplasticity", *Acta Metallurgica*, 35, 2983-2994.

[12] Moulinec, H., P. Suquet (1998), "Numerical method for computing the overall response of nonlinear composites with complex microstructure", *Computer Methods in Applied Mechanics and Engineering*, 157, 69-94.

[13] Mura, T. (1987), *Micromechanics of Defects in Solids*, Martinus-Nijhoff Publishers, Dordrecht.

[14] Ponte Castañeda, P. (1991), "The effective mechanical properties of nonlinear isotropic composites", *Journal of the Mechanics and Physics of Solid*s, 39, 45-71.

[15] Ponte Castañeda, P. (2002), "Second-order homogenization estimates for nonlinear composites incorporating field fluctuations: I- Theory", *Journal of the Mechanics and Physics of Solid*s, 50, 737-757.